AIChE WILEY InterScience DISCOVER SOMETHING GREAT

Viral Clearance Using Surfactant-Aided Size-Exclusion Chromatography

D. A. Horneman, M. Ottens, and L. A. M. van der Wielen
Dept. of Biotechnology, Delft University of Technology, Julianalaan 67, 2628 BC Delft, The Netherlands

J. T. F. Keurentjes
Process Development Group, Eindhoven University of Technology, 5600 MB, Eindhoven, The Netherlands

DOI 10.1002/aic.11145
Published online April 23, 2007 in Wiley InterScience (www.interscience.wiley.com).

Surfactant-aided size-exclusion chromatography (SASEC) is applied to the viral clearance of blood proteins, taking BSA as an example. Fixed bed systems as well as simulated moving bed (SMB) systems are examined. SASEC shows a better performance of this separation in terms of log reduction value (LRV), productivity of BSA, yield on BSA and solvent consumption compared to normal size-exclusion chromatography (SEC) in fixed bed as well as in SMB systems. © 2007 American Institute of Chemical Engineers *AIChE J,* 53: 1441–1449, 2007

Keywords: viral clearance, surfactants, size-exclusion chromatography, simulated moving bed, protein purification

Introduction

Biopharmaceutical products have to be free of possible viral contaminations. Virus contamination can arise from the source cell line or other biological starting material or by viruses introduced accidentally during the production process. One of the steps to assure the safety of the product is effective viral clearance during the purification process. Viral clearance can be achieved by either virus inactivation or virus removal. Examples of virus inactivation treatments are: heat treatment, irradiation, ethanol treatment, pH treatment, and solvent/detergent treatment.[1,2] Most of these treatments are effective for enveloped viruses. Nonenveloped viruses, however, often show higher physicochemical resistance.[3] When this resistance is broken, the treatment often results in the denaturation of the target product. Not all viruses can be inactivated with these methods. Therefore, each purification process must have at least one step that is effective in virus removal. Examples of purification steps that are also effective in virus removal are chromatographic techniques and filtration.[4,5] Of all chromatographic techniques, gel filtration or size-exclusion chromatography is not commonly known as an effective method for viral clearance. The main disadvantage of size-exclusion chromatography (SEC) is limited resolution, which can be increased only by increasing the column length or decreasing the sample load. Recently, it has been shown that selectivity and thus the resolution of SEC can be changed in situ, by using nonionic surfactants in the mobile phase[6–8] These nonionic surfactants form micelles at very low concentration. The manner in which biomolecules and bioparticles partition towards a phase containing "inert" micelles depends on the same parameters as in gel filtration chromatography: the volume fraction of micelles and the diameter ratio of solute and micelles. These parameters and thus the selectivity can be changed in situ by varying solution conditions, such as concentration and type of surfactants, temperature, and the addition of salts.[6–9]

This article demonstrates the application of surfactant-aided size-exclusion chromatography (SASEC) in viral clearance. As an example, the separation of BSA and bacteriophage ϕ29 is examined. BSA is used as a model for the human blood protein HSA. As a blood product, HSA can be contaminated by several viruses like HIV, hepatititus A virus

Correspondence concerning this article should be addressed to M. Ottens at m.ottens@tudelft.nl.

(HAV), hepatitis B virus (HBV), and hepatitis C virus (HCV).[10] These viruses have different sizes ranging from 20 to 150 nm. Bacteriophage $\phi 29$ has a size of about 42 nm[11,12] and represents a medium sized virus. The potential for viral clearance using SASEC is shown in both fixed bed and simulated moving bed chromatography.

Theory

Size-exclusion chromatography

The distribution coefficient in size-exclusion chromatography (SEC) is defined as the ratio of the solute concentration in the solid phase, $c_{i,s}$ over the solute concentration in the mobile phase, $c_{i,L}$ at equilibrium. Throughout this article, the solid phase is defined as the total gel volume, including the fibers and the pores of the gel particles.

$$K_i = \frac{c_{i,s}}{c_{i,L}} \tag{1}$$

In size-exclusion chromatography this distribution coefficient can be described by an excluded volume model that describes the steric interactions among the solutes and the fibers.[6,13,14] In this model, all volumes excluding a solute due to the presence of all types of fibers and solutes, including the solute itself, are calculated in each phase. The general equation[15] is given by:

$$K_i = \exp\left(-\sum_j \chi_{ij,s} + \sum_j \chi_{ij,L}\right) \tag{2}$$

where the dimensionless number $\chi_{ij,k}$ is the total excluded volume of solute i and a set of objects j per volume of phase k and is defined as:

$$\chi_{ij,k} = x_{i,k} U_{ij,k} \tag{3}$$

Where $\chi_{ij,k}$ is the number concentration of component j in phase k (#/m^3) and $U_{ij,k}$ is the excluded volumes between i and j in phase k. The excluded volume of two convex particles can be calculated using the following general expression[15,16]:

$$U_{ij} = V_i + \frac{S_i H_j + S_j H_i}{4\pi} + V_j \tag{4}$$

where V_i, S_i, and H_i are the volume, the surface area, and the integral of the mean curvature of component i, respectively. With this expression, it is possible to calculate the excluded volume between two convex objects of any shape or size.

Surfactant-aided size exclusion chromatography

In SASEC a non-ionic surfactant is added to the mobile phase above the critical micelle concentration. Now extra volume is excluded from a solute because of the presence of micelles. The distribution coefficient can again be predicted with equations 2–4. There is only one component extra in both phases: the micelle formed by the non-ionic surfactants. For example, when the micelle has an oblate shape, the distribution coefficient of a spherical solute i becomes:

$$K_i = \exp\left(\begin{array}{c} -\ln\left(\frac{1}{1-\phi_f}\right)\left(1+\frac{r_i}{r_f}\right)^2 - \left(\ln\left(\frac{1}{1-\phi_{m,s}}\right) - \ln\left(\frac{1}{1-\phi_{m,L}}\right)\right)\cdot \\ \left(1+\frac{1}{\eta_m}\left(\frac{r_i}{r_m}\right)^3 + \frac{3}{2}\left(\frac{r_i}{r_m}\right)^2 \frac{g(\eta_m)}{\eta_m} + \frac{3}{2}\left(\frac{r_i}{r_m}\right)\frac{f(\eta_m)}{\eta_m}\right) - \\ (\phi_{i,s} - \phi_{i,L})\cdot\left(1+\frac{r_i}{r_i}\right)^3 \end{array}\right) \tag{5}$$

with

$$f(\eta_m) = 1 + \eta_m^2(1-\eta_m^2)^{-1/2}\cosh^{-1}(\eta_m^{-1})$$

$$g(\eta_m) = \eta_m(1-\eta_m^2)^{-1/2}\cos^{-1}(\eta_m)$$

where r is the radius, ϕ is the volume fraction. The subscripts f and m indicate the gel fiber and the micelle. An oblate micelle is defined by three semiaxes r_m, r_m and $\eta_m r_m$ where $\eta_m < 1$. The concentration of micelles in the gel phase can be calculated using the distribution coefficient of the micelle itself. This distribution coefficient can again be calculated using Eqs. 2–4.[6] The last term describes the steric self-interaction among the protein molecules themselves in the solid and liquid phase. For dilute solute solutions this term, can be neglected.

Model description of concentration profiles in chromatography

Concentration profiles were simulated by numerical integration of the mass balance equations on the liquid and solid phase:

$$\frac{\partial c_{i,L}}{\partial t} = -v\frac{\partial c_{i,L}}{\partial z} + D_{ax}\frac{\partial^2 c_{i,L}}{\partial z^2} - \frac{1-\varepsilon}{\varepsilon}\frac{\partial c_{i,s}}{\partial t} \tag{6a}$$

$$\frac{\partial c_{i,s}}{\partial t} = k_0 a(c_{i,s}^{eq} - c_{i,s}) \tag{6b}$$

where v is the interstitial velocity, ε is the void fraction in the column, $k_o a$ is the overall mass transfer coefficient, calculated by:

$$\frac{1}{k_0 a} = \frac{d_p}{6}\left(\frac{K}{k_L} + \frac{1}{k_s}\right) \tag{7}$$

where k_L and k_s are the mass transfer at the liquid side and solid side respectively. These can be calculated from the Sherwood number. For the Sherwood number on the solid side a value of 10 is used.[13] K is the distribution coefficient, which depends on all actual volume fractions as is shown in Eq. 5. The liquid diffusion coefficient of BSA is $D_{BSA} = 6 \times 10^{-11}$ m^2/s.[17] The diffusion coefficient of bacteriophage is calculated from the Stokes-Einstein relation which gives $D_{\phi 29} = 5 \times 10^{-12}$ m^2/s. The intraparticle diffusion coefficient, D_s was calculated from these liquid diffusion coefficients[18]:

$$D_s = D_i \exp\left(-\phi_f^{0.5}\frac{r_i}{r_f}\right) \tag{8}$$

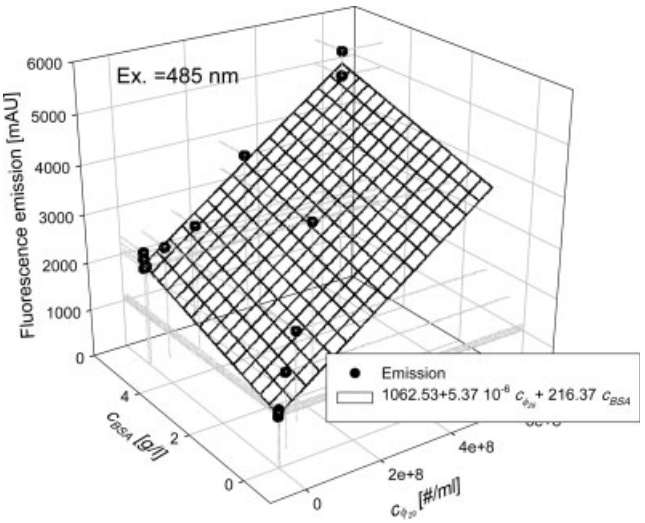

Figure 1. Fluorescence calibration curve for ϕ29 as function of the concentration of BSA.

For spatial discretization of the convection term, a second order backward discretization scheme was used. The axial dispersion was approximated by numerical dispersion.[19] The resulting system of ODEs is solved in time by a fourth order Runga-Kutta method.

Separation performance

The performance of the separation is described in terms of virus log reduction (*LRV*), yield of product (*Y*), productivity (*PR*), product concentration (c_{BSA}) and solvent consumption (*CS*). In the fixed bed experiments, these terms are defined as:

$$LRV = \frac{c_{\phi 29\_\mathrm{in}} V_{\mathrm{inj}}}{c_{\phi 29\_\mathrm{out}} V_{\mathrm{out}}} \tag{9}$$

$$PR = \frac{c_{\mathrm{BSA\_in}} V_{\mathrm{inj}} Y}{\Delta t_{\mathrm{cycle}} V_{\mathrm{s}}} \tag{10}$$

$$CS = \frac{\Delta t_{\mathrm{cycle}} \Phi}{c_{\mathrm{BSA\_in}} V_{\mathrm{inj}} Y} \tag{11}$$

where V_{inj} is the volume of the sample injected to the column, V_{out} is the volume collected as product, $\Delta t_{\mathrm{cycle}}$ is the cycle time, which is the time between two sample injections and Φ is the flow rate.

In the SMB experiments, these terms are defined as:

$$LRV = \frac{c_{\phi 29,\mathrm{F}} \Phi_F}{c_{\phi 29,E} \Phi_E} \tag{12}$$

$$PR = \frac{c_{\mathrm{BSA,F}} \Phi_{\mathrm{F}} Y}{V_{\mathrm{s}}} \tag{13}$$

$$CS = \frac{\Phi_D}{c_{\mathrm{BSA,F}} \Phi_{\mathrm{F}} Y} \tag{14}$$

Where the subscripts D, F, and E stand for desorbent, feed, and extract.

Materials and Methods

Fixed bed experiments

Column. An Omnifit column from BioRad was used in a FPLC Äkta Explorer (GE Healthcare). The column was packed with Sephacryl™ S300 HR (Amersham Biosciences BV, cat. no. 17-0599-01) up to a height of 6.7 cm. The volume fraction of the gel fibers, ϕ_{f}, has been determined from the responses to salt pulses. Small salt molecules (NaCl) can diffuse into all the pores of the gel. The difference between the elution volume of NaCl and the geometrical volume of the column gives the volume of the gel fibers. A value of 0.08 was found for this gel, the radius of the gel fiber, r_{f} was assumed to be 1.5 nm.[6] The dead volume of the system (total volume between injection point and spectrophotometer minus the column volume itself) is determined by pulses of dextran blue and BSA. The void volume of the packed column is determined by dextran blue pulses.

Experiments. Pulses of 0.5 ml containing 2.5 g/l BSA (Sigma, cat. no A 7906) and about 1.5×10^9 phages/ml (DSMZ, DSM 5546) in a surfactant-buffer solution were injected. In all experiments, a 10-mM phosphate buffer, pH 6.8 containing 0.1 M NaCl and a known concentration of surfactant was used as eluent. The flow was kept constant at 1 ml/min. The surfactant used in these experiments was the non-ionic surfactant $C_{12}E_{23}$ (Acros organics, cat. no 228345000). Various surfactant concentrations between 0 and 20% (w/w) were used in the eluent.

Analyses. The samples were collected using a fraction collector (Frac-920, GE Healthcare). The protein concentration was determined off-line by a spectrophotometer (Ultrospec 2000, GE Healthcare) at 280 nm. The concentration of phages was determined using a PicoGreen® dsDNA quantification reagent (Molecular Probes, p11496). This is a fluorescent nucleic acid stain for quantification of double stranded DNA in solution. The samples were excited at 485 nm and the fluorescence emission intensity was measured at 520 nm using a fluorescence microplate reader (Tecan). A calibration curve was made, which also included the effect of the concentration of BSA on the analysis (Figure 1).

SMB Experiments

Equipment. An 8-column carousel SMB was used for the SMB experiments. The SMB consisted of three sections with respectively 3, 3, and 2 columns (see Figure 2). In total 3 Shimadzu LC-8A pumps were used for the desorbent, feed, and extract flow. The actual flow rates were determined by monitoring the change in weight during the experiment using

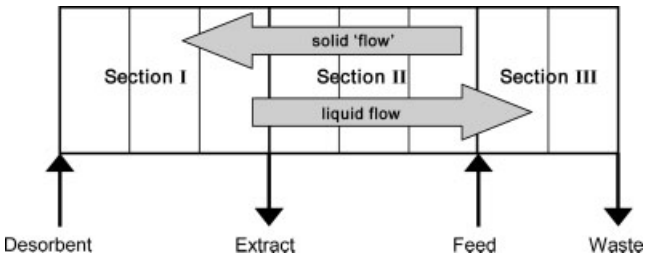

Figure 2. SMB setup used in the experiments.

Table 1. K-Values of phi29 and BSA at Different surfactant concentrations

c_{C12E23}, % (w/w)	$K_{\phi 29}$[-]	K_{BSA}*[-]
0	0	0.39
2.5	0	N.A.
5	0	0.51
7.5	0	0.63
10	0	0.67

*Data taken from[6].

Mettler Toledo balances (PG-S). The concentration of surfactant in the extract waste outlet was monitored by a Shimadzu UV-VIS detector (SPD-10AV) at 280 nm.

Columns. The in-house made stainless steel columns had a diameter of 2 cm and a length of 10 cm. The columns were packed with Sephacryl S300 HR (GE Healthcare, cat no. 17-0599-01) at 3 ml/min for 1 h followed by a flow rate of 12 ml/min for 3 h. The reproducibility of the packing procedure was checked by pulse experiments with dextran blue. The void volume was determined from the same pulse experiments. An average void fraction of 0.4 ± 0.02 was found for each column.

Experiments. Before each experiment, the columns were "regenerated" with a 10 mM phosphate buffer, pH 6.8, containing 0.15 M NaCl. After this step the feed inlet was changed to a 5 g/l BSA solution without ϕ29. When the BSA concentration profile was constant in the SMB, the feed was changed again to a 5g/l BSA solution containing the bacteriophage ϕ29. In the experiments with a surfactant gradient, the gradient was first positioned before the feed was changed to a BSA solution.

To measure the concentration profile in the SMB system, samples were taken at the inlet of one of the columns exactly halfway each switch-interval of the columns. To take the samples, an injection valve with a sample loop was placed before this column. At the time of sampling the sample loop was disconnected from the main flow path. The sample loop, filled with the sample, was emptied by injecting air in the sample loop. The sample loop was then loaded again with buffer and reconnected within the main flow path. The volume of the sample loop was only 0.3 ml, and taking samples had no effect on the experimental profiles.

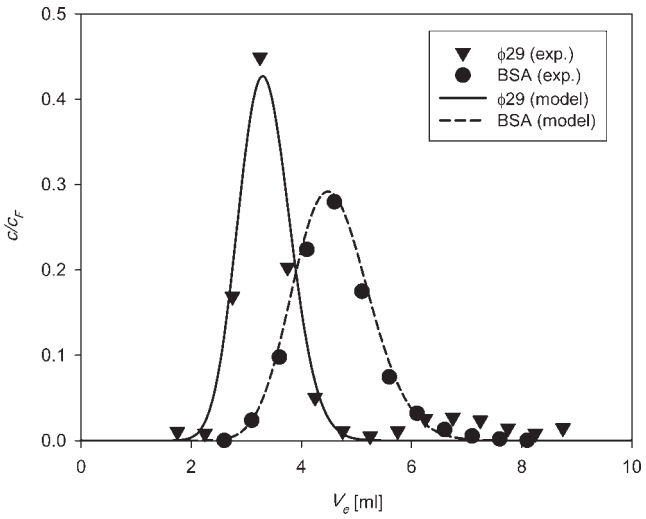

Figure 3. Elution profiles of ϕ29 and BSA at 0% (w/w) of $C_{12}E_{23}$.

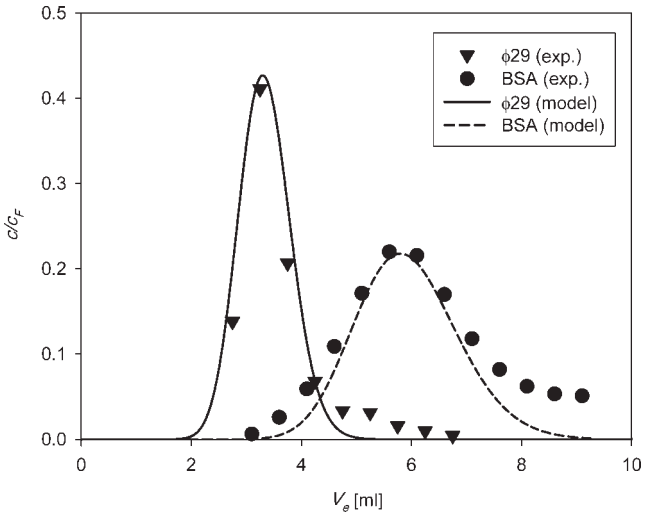

Figure 4. Elution profiles of ϕ29 and BSA at 10% (w/w) of $C_{12}E_{23}$.

Results and Discussion

Fixed bed experiments

The influence of $C_{12}E_{23}$ on the distribution behavior of BSA has been described previously.[6] The influence of the same surfactant on the bacteriophage ϕ29 has been determined by pulse experiments using different surfactant concentrations in the mobile phase. Table 1 shows that although the micelle concentration influences the distribution behavior of BSA, it does not influence the behavior of ϕ29. The diameter of ϕ29 is in the range of 42–60 nm,[20] which is larger than the pore size of S300, which is 13 nm.[21] Diffusion of ϕ29 into the pores is thus not possible.

Resolution. With a K-value of 0 for ϕ29, the selectivity is excellent. The resolution, however, determines how good the separation really is. This resolution is dependent on the difference in retention volumes and on the width of both

Table 2. Comparison of Yield (*Y*), Productivity (*PR*) and Solvent Consumption (*CS*), Log Reduction Value (*LRV*) Using SEC (First and Third Column) and SASEC (Second and Last Column)

	Comparison at $Y = 0.85$		Comparison at $LRV = 3.21$	
	SEC	SASEC	SEC	SASEC
$c_{C_{12}E_{23}}$, %, (w/w)	0	10	0	10
Y	**0.85**	**0.85**	0.26	0.85
PR, g BSA/10^{-3}m^3/d	25.1	20.08	7.5	20.08
CS, l/g BSA	10.74	13.42	35.8	13.42
LRV	0.87	3.21	**3.21**	**3.21**
c_{BSA}, g/l	0.2	0.16	0.09	0.16

Table 3. Constraints for the Flow Ratios for Positioning a Gradient of $C_{12}E_{23}$ and the Separation of BSA and phi29

Gradient	Front	Front Shape	m
Upward	1	Shock	$\left(\frac{\Delta q}{\Delta c}\right)_{c_{III}-c_D}, K_{BSA} < m_I; \left(\frac{\partial q}{\partial c}\right)_{c_{III}-c_D}, K_{\phi 29} < m_{II} < K_{BSA}$
	2	Diffuse	$\left(\frac{\partial q}{\partial c}\right)_{c_{III}}, K_{\phi 29} < m_{III} < K_{BSA}$
Downward	1	Diffuse	$K_{BSA} < m_I < \left(\frac{\partial q}{\partial c}\right)_{c_{II}}; K_{\phi 29} < m_{II} < \left(\frac{\partial q}{\partial c}\right)_{c_{II}}, K_{BSA}$
	2	Shock	$K_{\phi 29} < m_{III} < \left(\frac{\Delta q}{\Delta c}\right)_{c_{II}-c_D}, K_{BSA}$

response curves.

$$R = \frac{V_{e2} - V_{e1}}{\frac{1}{2} \cdot (W_1 + W_2)} \tag{15}$$

where V_e is the elution volume and W_i is the width of pulse i. These response curves are influenced by the K-value but also by the length of the column, flow rate, sample size and mass transfer characteristics.[22] In conventional SEC, a high resolution can be obtained only by increasing column length or decreasing the flow rate or the sample load. All these changes will also result in reduced performance in terms of yield, productivity, solvent consumption and/or product concentration. SASEC is a tool to influence the resolution by changing the K-values, by changing only the solvent conditions. This is demonstrated by the separation of BSA and ϕ29. Figures 3 and 4 show the pulse response curves in case of surfactant concentrations of 0 and 10% (w/w) in the mobile phase, respectively.

At 0% (w/w) the resolution is equal to 0.5. Addition of 10% (w/w) of surfactant to the mobile phase increased the resolution to a value of 1. This higher resolution indicates that a higher *LRV* can be achieved with the same yield on BSA. Table 2 shows the differences in performance of the experiments. In the first two columns, a comparison is made at a yield of 85%. At this yield a substantially higher *LRV* is reached with SASEC. The *LRV* with SEC is actually below 1, which cannot be considered as virus removal. Although the productivity is less and the solvent consumption is higher with SASEC than with SEC, this is attributable to the increase in cycle time in SASEC.

The last two columns of Table 2 show the differences in performance at a *LRV* of 3.21. To reach this *LRV*-value in SEC, only a small fraction of BSA can be collected. As a result, the productivity and yield decrease and the solvent consumption increases substantially.

Concentration of BSA. Addition of surfactant to the mobile phase does not significantly effect the product concentration of BSA. It remains diluted in both cases. In order to also solve this problem, SASEC-SMB should be used.

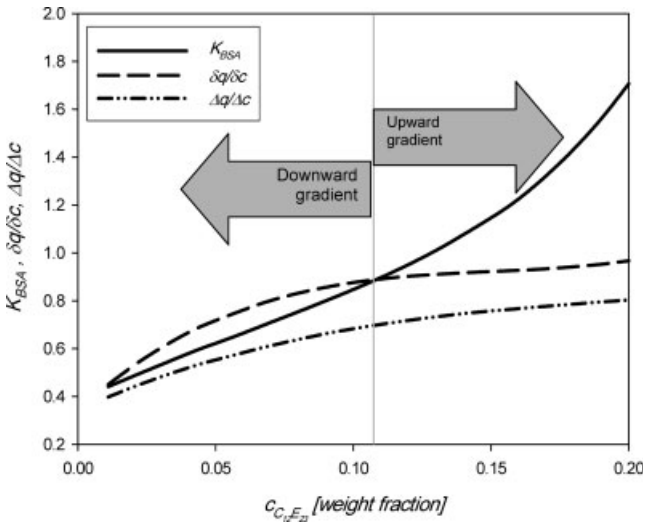

Figure 5. Distribution behavior of BSA and $C_{12}E_{23}$ as function of the concentration of $C_{12}E_{23}$.

SMB experiments

Area of separation. The SMB used in this article contains only three sections (Figure 2). In Section 2 and 3 separation takes place, while in Section 1 BSA is eluted. Normally a fourth section is used to retain the other component at the other side of the SMB. In this article however this other component is ϕ29 and cannot be retained because it is too large to enter the pores of the gel particles. Therefore Section 4 is omitted in this SMB.

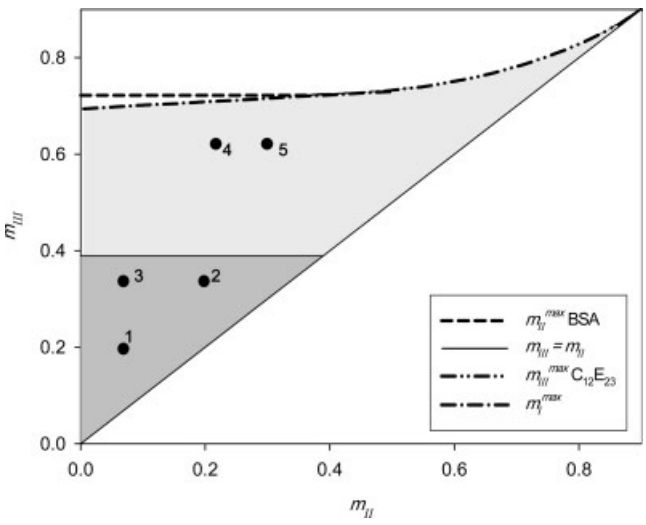

Figure 6. Area of separation for BSA and ϕ29 in SEC-SMB (dark gray area) and area of separation in SASEC-SMB (light and dark gray area).

The dots give the m-values of the experiments.

Table 4. Parameters Used During the SMB Experiments

Exp.	m_I	m_{II}	m_{III}	Φ_D, [ml/min]	Φ_E, [ml/min]	Φ_F, [ml/min]	τ, [s]	c_D, [% w/w]
1	0.40	0.05	0.20	7.0	2.2	1.0	180	0
2	0.40	0.20	0.35	7.0	1.3	1.0	180	0
3	0.40	0.05	0.35	3.8	1.2	1.0	330	0
4	0.54	0.20	0.60	3.2	0.9	1.0	450	9.5
5	0.60	0.30	0.60	4.3	1.0	1.0	345	9.5

The optimal way to use the concept SASEC in an SMB is by using a surfactant gradient that has used in a low surfactant concentration in the Sections 1 and 2 and a high concentration in Section 3. In this way the loading capacity of BSA will be increased in Section 3 while a low surfactant concentration in Section 1 and 2 facilitates the elution of BSA in these sections. Two types of gradients can be formed: an upward gradient, in which the surfactants are predominantly transported with the liquid flow, or a downward gradient in which the surfactant is predominantly transported with the solid phase[23] The constraints for separation in both cases are given in Table 3. The derivation of these constraints is given elsewhere.[24] In this article the surfactant used is $C_{12}E_{23}$. This surfactant forms oblate shaped micelles that can be described by two radii of 4.13 and 3.66 nm, respectively.[6] The micelles formed have a concave curved isotherm. This type of isotherm results in a shock front during loading of the column with a solution with increased surfactant concentration and a diffuse front during elution with a solution with a decreased surfactant concentration.

Figure 5 shows the distribution behavior of this surfactant compared to the behavior of BSA and ϕ29. In combination with the constraints in Table 3 it can be seen that below 11 wt % of surfactant a downward gradient should be chosen. Above this concentration an upward gradient should be chosen. To prevent high viscosities in the SMB, a downward gradient is chosen. For all experiments the surfactant concentration in the desorbent was set to 9.5 wt %. With the constraints given in Table 3, the area of separation is constructed at this desorbent concentration. This area of separation is given in Figure 6. The line m_I^{max} gives the m_{III} and m_{II} val-

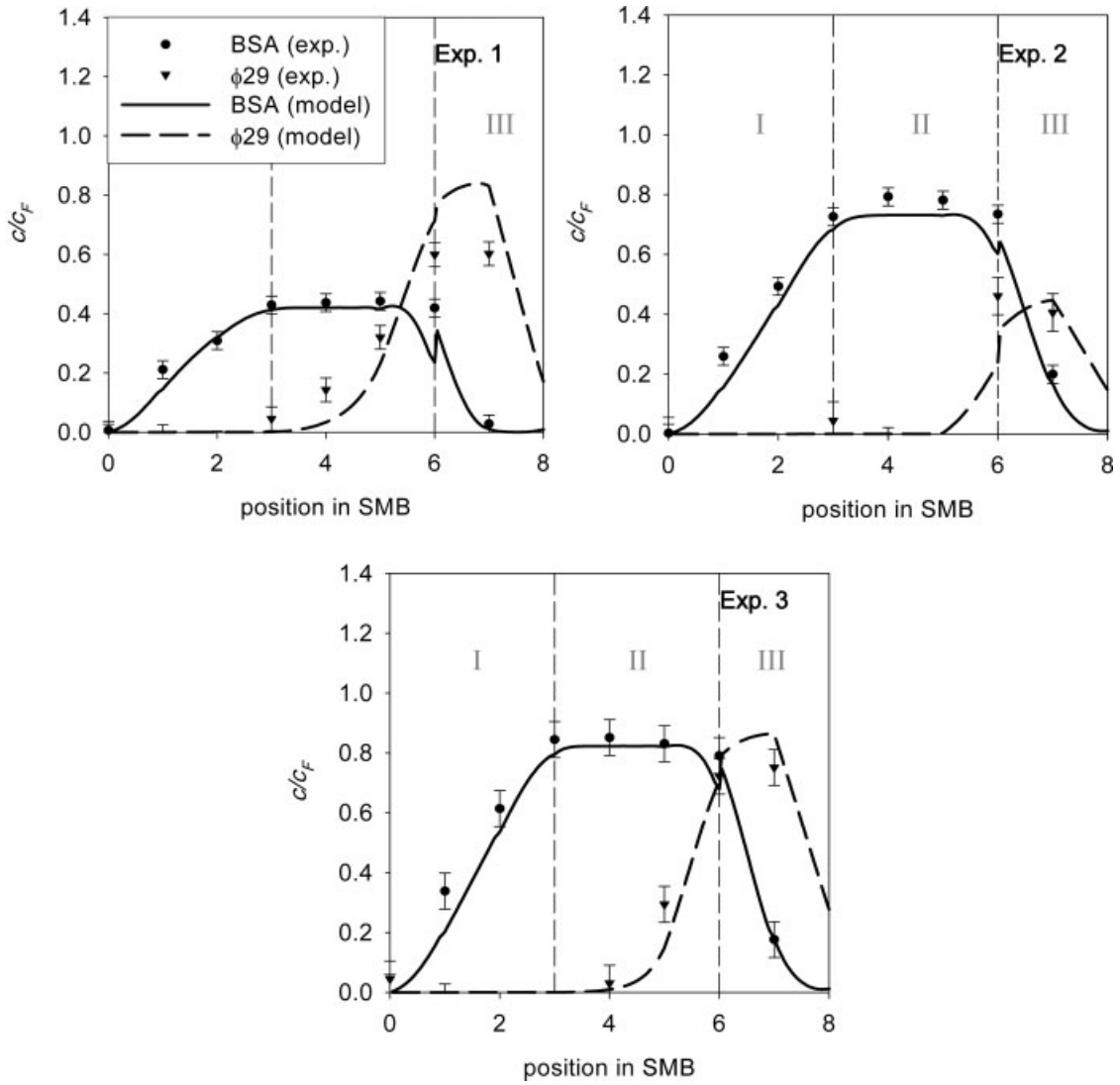

Figure 7. Concentration profiles of BSA and ϕ29 in the SEC-SMB experiments 1, 2 and 3.

Table 5. Performance of the SMB Experiments

Exp.	*LRV*	*Y*	*PR*, [g BSA/10^{-3}°m^3 (gel)/d]	*CS*, [l/g BSA]	c_{BSA}, [c/c_F]
1	2.7	0.92	22.0	1.5	0.41
2	11.1	0.88	21.0	1.6	0.68
3	3.8	0.95	22.7	0.79	0.79
4	12.3	0.98	23.3	0.65	1.1
	16.9	0.96	23.0	0.93	0.96

ues at which the concentration of surfactant in Section 2 becomes such that $K_{BSA} = \delta q/\delta c$. Above this line the constraint for m_I cannot be fulfilled. The boundary of m_{III} is further only depending on the constraints of $C_{12}E_{23}$, because $K_{BSA} > \left(\frac{\Delta q}{\Delta c}\right)_{c_{II}-c_D}$ as can be seen in Figure 5. In the same way it can be seen that m_{II} is dependent only on the constraint of BSA because $K_{BSA} < \left(\frac{\partial q}{\partial c}\right)_{c_{II}}$. The dark gray area in Figure 6 represents the area of separation for the case that no surfactants are used. From comparison of these two areas it can already be seen that a higher productivity is possible in SASEC-SMB compared to SEC-SMB

The *m*-values chosen for the experiments are also given in Figure 6. Table 4 also gives these *m*-values together with the flow rates and switch times of the experiments. The feed flow has been kept constant in each experiment for ease of comparison.

SEC-SMB

Log reduction. The measured concentration profiles in the SMB are given in Figure 7. From this figure it can be seen that the extent of viral clearance is mainly determined by the value of m_{II}. An increase of m_{II} causes the ϕ29 concentration profile to move more towards the right. A better clearance is thus achieved. The phages are too large to enter the pores of the gel material and will thus only move with the mobile phase. At larger flows this movement is faster and more ϕ29 is removed with the waste stream. The dynamic model describes the concentration profiles very well. The model has been used to determine the log reduction that can be achieved in the extract (product) flow. These log reductions are given in Table 5.

BSA concentration The maximal possible concentration of BSA is determined by:

$$C_{BSA,E}^{max} = \frac{m_{III} - m_{II}}{m_I - m_{II}} \cdot C_{BSA,F} \tag{16}$$

This can be achieved only when the yield on BSA is 1. Concentrating the product is therefore only possible when m_I has a lower value than m_{III}. This is however not possible in isocratic SMB due to the constraints of the *m*-values (see Table 3). An m_I-value close to the m_{III} value will thus give the highest possible concentration. In the first three experiments the m_I-value has been kept constant. It can be seen from the figures that the concentration in the extract is indeed increasing when m_{III} is increased. Concentration of the product is, however, not possible in an isocratic mode.

SASEC SMB

Log reduction. In the isocratic surfactant-free experiments, it was found that an increase in m_{II} results in an increase in log reduction. When surfactants are introduced in the desorbent flow, higher m_{II}-values can be chosen (Figure 6). Two experiments have been performed at $c_D = 9.5\%$ (w/w), the results can be seen in Figure 8. The model predicts a better clearance compared to SEC-SMB and the experimental results confirm this to a limited extent. In the fixed bed experiments no influence of surfactant was found on the distribution behavior of ϕ29. The bacteriophage cannot enter the pores of the gel and will thus be moved with liquid flow. The experimental results in the SASEC experiments, however, seem to show a larger deviation from the model prediction than the other experiments. This can be explained by several reasons. The concentration of ϕ29 in the last two experiments was twice as low as in the first three

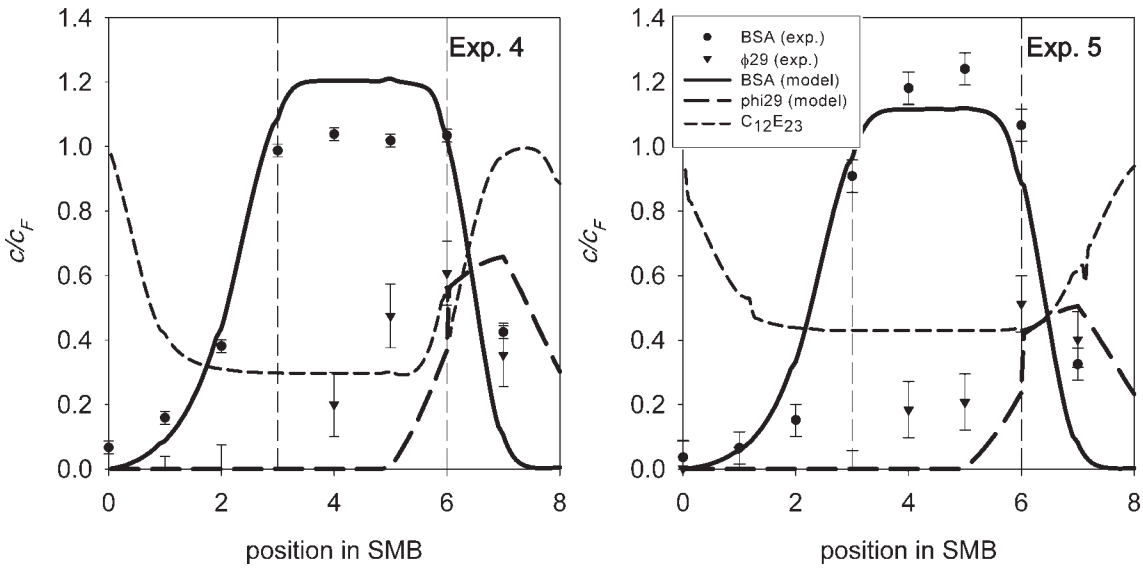

Figure 8. Concentration profiles of BSA and ϕ29 in the SASEC-SMB experiments 4 and 5.

experiments. In the figures a relative concentration is given. The concentration of ϕ29 in Section 2 was thus in the lower range of the detection limit and the error is larger in this range. It is also possible that the signal was the results of naked DNA from phages broken apart. Finally, the presence of surfactant can also influence the fluorescence measurements, which was not taken into account.

BSA concentration. Due to the surfactant gradient, it is now possible to choose a m_I that is equal to or even lower than m_{III}, meaning that concentration of BSA should be possible. This is indeed the case in our experiments as can be seen in Figure 8.

Solvent consumption. In all experiments the feed flow has been kept constant at 1 ml/min. This makes it easy to compare the desorbent flows of each experiment. In experiment 2 and 4 the same m_{II} value has been used. The advantage of the SASEC experiment is besides the increase of BSA concentration the decrease in desorbent flow with almost a factor 2.

Productivity. The productivity does not seem to change much using SASEC-SMB instead of SEC-SMB. The reason is that for all experiments the same amount of gel has been used and the same feed flow. The productivity is thus only depending on the yield of the process (see Eq. 14). In experiment 2 the yield is significantly lower than in the SASEC-experiments, because BSA is lost via the waste stream. To prevent this loss, more column length is needed in Section 3. This will negatively influence the productivity. In experiments 1 and 3, the yield is about the same as that in the SASEC experiments, but the achieved *LRV*-values are much lower. To get the same *LRV*-values as in the SASEC experiments, more column length is needed in Section 2. This will also result in lower productivity. The SASEC experiments, however, show both high yield and high *LRV*-values. Probably, in practice, lower *LRV*-values are already sufficient which means that a smaller bed length in Section 2 can be used. In that case even higher productivity can be achieved with SASEC-SMB.

Conclusion

The separation of BSA and ϕ29 is performed using traditional SEC and using surfactant-aided SEC, SASEC. Pulse experiments in fixed bed chromatography showed that with SASEC the protein BSA was more distributed towards the solid phase than compared to using SEC. The micelles had no influence on the distribution behavior of ϕ29. Therefore, higher resolution could be achieved when using SASEC. The experimental results were in good agreement with the dynamic model, presented in this article. This model uses the excluded volume theory to describe the distribution behavior of solutes between the mobile phase and solid phase in the presence of (non-ionic) micelles. Experiments and model showed that when using SASEC, larger *LRV*-values could be achieved than with SEC without loss of productivity or increase in solvent consumption.

Even larger *LRV*-values and lower solvent consumption can be achieved using the SASEC principle in simulated moving bed. The SMB-experimental results were in good agreement with the model. Evaluation of the results showed that higher productivity could be achieved with SASEC-SMB compared to SEC-SMB based on resin volume. Another advantage of SASEC-SMB is the absence of product dilution. As a matter of fact, it is possible to concentrate the product, which is not possible with normal SEC-SMB.

The complete validation of SASEC and its practical implications for GMP operation is a matter for future research. This article, however, shows the potential and advantages of SASEC in viral clearance.

Notation

$c_{i,k}$ = concentration of solute i in phase k
CS = solvent consumption
D = diffusion coefficient
D_{ax} = dispersion coefficient
d_p = particle diameter
H_i = integral of mean curvature of component i
K_i = distribution coefficient of component i
k_L = mass transfer coefficient at liquid side
$k_o a$ = overall mass transfer coefficient
k_s = mass transfer coefficient at solid side
LRV = log reduction value
m_j = flow ratio in section j
PR = productivity
r_i = radius of component i
R = resolution
S_i = surface area of component i
t = time
U_{ij} = excluded volume between components i and j
v = interstitial velocity
V_e = elution volume
V_i = volume of component i
V_{inj} = injected volume
V_{out} = collected volume
W_i = peak width
x_i = number concentration of component i
Y = yield
z = distance

Greek letters

Φ = flow
ε = column void fraction
ϕ_i = volume fraction of component i
γ_{ij} = steric interaction parameter between components i and j
$\eta_m r_m$ = semi-axis of oblate micelle
Δt_{cycle} = cycle time

Sub and superscripts

D = desorbent
E = extract
eq = equilibrium
F = feed
f = gel fiber
L = liquid phase
m = micelle
s = solid phase
I,II,III = section number in SMB

Literature Cited

1. Burnouf T, Griffiths E, Padilla A, Seddik S, Stephano MA, Gutiérrez JM. Assessment of the viral safety of antivenoms fractionated from equine plasma. *Biologicals*. 2004;32:115–128.
2. Kalyanpur M. Downstream processing in the biotechnology industry. *Mol Biotech*. 2002;22:87–98.
3. FDA. *Guidance on viral safety evaluation of biotechnology products derived from cell lines of human or animal origin*, Food and Drug Administration, Rockville, MD, 1998.

4. Levy RV, Phillips M, Lutz H. *Filtration in biopharmaceutical Industry*. New York: Marcel Dekker, 1998
5. Burnouf T, Radosewich M. Nanofiltration of plasma-derived biopharmaceutical products. *Haemophilia*. 2003;9:24–37.
6. Horneman DA, Wolbers M, Zomerdijk M, Ottens M, van der Wielen LAM. Surfactant aided size exclusion chromatography. *J Chromatogr B*. 2004;807:39–45.
7. van Roosmalen D, Lazzara MJ, van den Broeke LJP, Keurentjes JTF, Blankschtein D. Protein partitioning driven by excluded-volume interactions in an aqueous nonionic micellar-gel system. *Biotech Bioeng*. 2004;87:695–703.
8. Horneman DA, Ottens M, van den Broeke LJP, van Roosmalen D, Keurentjes JTF, van der Wielen LAM. *Separation method for bioparticles*. STW, Utrecht (NL): Aanvrager, 2004 No EP1491246.
9. Evans DF, Wennerström H. *The Colloidal Domain*. New York: VCH, 1994
10. Adcock WL, MacGegor A, Davies JR, Hattarki M, Anderson DA, Goss NH. Chromatographic removal and heat inactivation of hepatitis A virus during manufacture of human albumin. *Biotechnol Appl Biochem*. 1998;28:85–94.
11. Meijer WJJ, Horcajada JA, Salas M. φ 29 family of phages. *Microbiol Mol Biol Rev*. 2001;65:261–287.
12. Anderson DL, Hickman DD, Reilly BE. Structure of bacillus subtillus bacteriophage φ29 and length of φ29 deoxyribonucleic acid. *J bacteriol*. 1966;91:2081–2089.
13. Bosma JC, Wesselingh JA. Partitioning and diffusion of large molecules in fibrous structures. *J Chromatogr B*. 2000;743:169–180.
14. Ogston G. The spaces in a uniform random suspension of fibres. *Trans Faraday Soc*. 1958;54:1754–1757.
15. Lazzara MJ, Blankschtein D, Deen WM. Effects of multisolute steric interactions on membrane partition coefficients. *J Colloid Interface Sci*. 2000;226:112–122.
16. Jansons KM, Phillips CG. On the application of geometric probability theory to polymer networks and suspensions. *J Colloid Interface Sci*. 1990;137:75–91.
17. Sober HA. editor. *CRC Handbook of Biochemistry: Selected Data for Molecular Biology*, 2nd ed. Cleveland, Ohio: The Chemical Rubber Co., 1970
18. Vonk P. *Diffusion of Large Molecules in Porous Structures*, Doctoral thesis. Groningen: University of Groningen, 1994
19. Guiochon G, Golshan Shirazi S, Katti AM. *Fundamentals of Preparative and Non-Linear Chromatography*. Boston: Academic Press, 1994.
20. van Regenmortel MHV, Fauquet CM, Bishop DHL, Carstens EB, Estes MK, Lemon SM, Maniloff J, Mayo MA, McGeoch DJ, Pringle CR, Wickner RB, editors. The seventh report of the International Committee on Taxonomy of viruses. San Diego: Academic Press, 2000
21. Hagel L, Ostberg M, Andersson T. Apparent pore size distributions of chromatography media. *J Chromatogr A*. 1996;743:33–42.
22. Giddings JC. *Dynamics of Chromatography*. New York: Marcel Dekker, 1965
23. Houwing J, Billiet HAH, van der Wielen LAM. Mass transfer effects during separation of proteins in SMB by size exclusion. *AICHE J*. 2003;49:1158–1167.
24. Horneman DA, Ottens M, van der Wielen LAM, Keurentjes JTF. Micellar gradients in size-exclusion simulated bed chromatography. *J Chromatogr A*. 2006;1113:130–139.

Manuscript received Jan. 4, 2006, and revision received Jan. 21, 2007.